Journal of Applied Spectroscopy, Vol. 91, No. 3, July, 2024 (Russian Original Vol. 91, No. 3, May–June, 2024)

TRANSFER OF ELECTRONIC EXCITATION ENERGY BETWEEN THIOFLAVIN *T* AND ITS STYRYL DERIVATIVES INCORPORATED INTO AMYLOID FIBRILS

E. I. Pligin,[a] A. A. Lugovski,[b] E. S. Voropay,[b] and A. A. Maskevich[a,*]

UDC 535.371/547.681:547.458.68

The spectral and luminescent properties of the styryl derivative of thioflavin T (ThT) 2-{(1E,3E)-4-[4-(dimethylamino) -2,6-dimethylphenyl]buta-1,3-dien-1-yl}-3-ethyl-1,3-benzothiazolium-3 tosylate (Th-C23) were studied. The fluorescence decay kinetics of Th-C23 incorporated into amyloid fibrils (AF) were not exponential and could be represented as a unimodal distribution of fluorophores over duration α(t). ThT and Th-C23 were shown to form an effective donor–acceptor (D–A) pair when incorporated into the AF structure. The degree of polarization of the acceptor fluorescence was high (~0.4) within the entire spectrum, despite the energy transfer, and was explained by the special orientation of D–A pairs, parallel and antiparallel. The measured fluorescence spectrum of the donor (ThT) and absorption spectrum of the acceptor (Th-C23) were used to calculate the critical energy-transfer radius R_0, which could take values from 54 to 68 Å depending on the mutual orientation and quantum yield of the donor and acceptor.

Keywords: *thioflavin T, styryl derivatives of thioflavin T, fluorescence decay kinetics, time-resolved fluorescence, amyloid fibrils, Forster resonance energy transfer, maximum entropy method.*

Introduction. A strong dependence of the quantum yield and fluorescence decay time on the microenvironment viscosity is a feature of the spectral properties of fluorescent molecular rotors (MRs) [1–4]. These properties of MRs are responsible for their broad application as viscosity and temperature sensors in locally microscopic volumes [5, 6]. The use of MRs to detect and study the formation mechanism of amyloid fibrils (AF) is one of their most important applications [7–10]. The benzothiazole dye thioflavin T (ThT), which also exhibits MR properties [3], is traditionally used to study AF. Efforts to adapt MRs to studies of AF are directed at improving their optical properties, particularly the design of dyes that absorb and fluoresce in the red and near-IR spectral regions, and at increasing their specificity. For this, a series of styryl derivatives of benzothiazole, many of which possess MR properties, were recently synthesized [11–15]. One such compound is a styryl derivative of ThT, i.e., 2-{(1*E*,3*E*)-4-[4-(dimethylamino)-2,6-dimethylphenyl)buta-1,3-dien-1-yl]-3 -ethyl-1,3-benzothiazolium-3 tosylate (Th-C23). Previously, this dye was found to have long-wavelength absorption and fluorescence spectra (520 and 600 nm) [15]. Quantum-chemical calculations and experimental studies showed that Th-C23 was an MR. As a result, its fluorescence quantum yield in low-viscosity solvents was low (~10^{-4}), which increased by greater than three orders of magnitude upon incorporation in AF.

The present work investigated the spectral properties of Th-C23 in solution and its complex with AF. This dye in combination with ThT was shown to be useful as a donor–acceptor pair to study the structure and properties of AF.

Experimental. Absorption spectra of solutions were measured using a Specord 200 PC spectrophotometer (Carl Zeiss, Germany); fluorescence spectra, a CM 2203 spectrofluorimeter (Solar, Belarus). Fluorescence decay lifetimes were measured on a locally fabricated laboratory system operating in time-resolved single-photon counting mode [16]. Fluorescence decay curves were analyzed using software written at Y. K. State University of Grodno [17, 18]. Experimental fluorescence decay curves of Th-C23 were analyzed using a model of discreet and continuous fluorophore distributions over emission time. In the first instance, the fluorescence decay function $F(t)$ was written as the sum of several exponentials:

*To whom correspondence should be addressed.

[a]Yanka Kupala State University of Grodno, Grodno, Belarus; email: amaskevich@grsu.by; [b]Belarusian State University, Minsk, Belarus. Translated from Zhurnal Prikladnoi Spektroskopii, Vol. 91, No. 3, pp. 344–351, May–June, 2024. Original article submitted January 18, 2024.

$$F(t) = \sum_{i=1}^{n} \alpha_i \exp(-t/\tau_i),$$

where α_i and τ_i are the amplitude and duration of the decay of the *i*th component; *n*, the number of exponentials.

The contribution of an individual component to the fluorescence decay was determined using the formula $S_i = \tau_i/\Sigma\alpha_i\tau_i$.

The function $F(t)$ for modeling a continuous distribution over emission decay times was written

$$F(t) = \int_0^{\infty} \alpha(\tau) \exp\left[-t/\tau\right] d\tau,$$

where $\alpha(\tau)$ is a certain continuous function. Distribution $\alpha(\tau)$ was defined using the maximum entropy method (MEM) [18, 19].

The quantity χ^2 ($\chi^2 \leq 1$) served as a quality criterion along with the random distribution of weighted residuals relative to the time axis:

$$\chi^2 = \frac{1}{N} \sum_{i=1}^{N} W_i \left[I_e(t_i) - I(t_i)\right]^2, \quad R(t_i) = \left[I_e(t_i) - I(t_i)\right],$$

where W_i are weighting factors; *N*, total number of experimental points. The calculated function $I(t)$ resulted from convolution of the sample decay function $F(t)$ with the instrument function $I(t)$.

Th-C23 had the structure

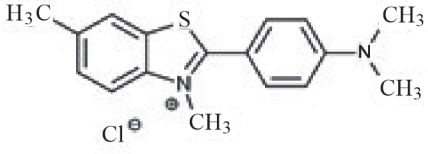

ThT

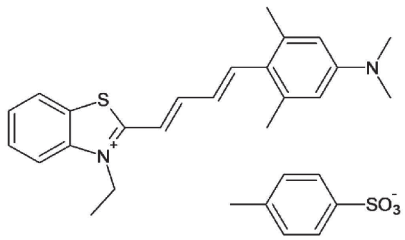

Th-C23

and was synthesized at the Department of Laser Physics, BSU, by Docent A. A. Lugovski. The structure of the synthesized compound was confirmed using NMR and mass spectroscopy. PMR spectra were recorded in CD_3CN on a Bruker AC 500 spectrometer at operating frequency 500 MHz. Mass spectra were recorded using an Agilent 1200 Rapid Resolution LC liquid chromatograph with an Agilent 6410 Triple Quad mass detector. A solution of the dye (1 mg) in MeCN (1 mL) was injected into the analyzer.

AF were prepared from bovine insulin (Sigma, USA) by the standard method [20].

Results and Discussion. *Th-C23 fluorescence decay kinetics in the presence of AF in solution.* Nonexponential kinetics are a feature of MR fluorescence decay [21, 22]. The reason for this is the nonequilibrium nature of the emitting state because of torsional and solvation relaxation associated with it. An analysis of Th-C23 fluorescence decay kinetics (λ_{ex} = 467 nm, λ_{fl} = 600 nm) with the decay function represented as the sum of exponentials produced the following parameters: $\alpha_1 = 0.750$, $\tau_1 = 0.07 \pm 0.01$ ns, $S_1 = 36.6\%$; $\alpha_2 = 0.237$, $\tau_2 = 0.33 \pm 0.01$ ns, $S_2 = 52.0\%$; $\alpha_3 = 0.013$, $\tau_3 = 1.30 \pm 0.04$ ns, $S_3 = 11.4\%$; $\langle\tau\rangle = 0.35 \pm 0.04$ ns, $\chi^2 = 1.16$. The kinetics were nonexponential and could be approximated well ($\chi^2 \approx 1$) as the sum of three exponential terms, despite the limitation of relaxation processes upon incorporation into AF. It was assumed that the complex nature of the fluorescence decay kinetics was due to the heterogeneous microenvironment of the Th-C23 molecules, i.e., dye molecules that were situated in a rigid microenvironment and the torsional relaxation of which was limited had a long fluorescence decay time.

Representation of the decay function of heterogeneous systems such as AF as the sum of several exponentials is formal because it is often difficult to assign a definite meaning to individual components. In this instance, the decay function can be adequately modeled as a continuous distribution of fluorophores over emission decay times [18]. Figure 1 illustrates

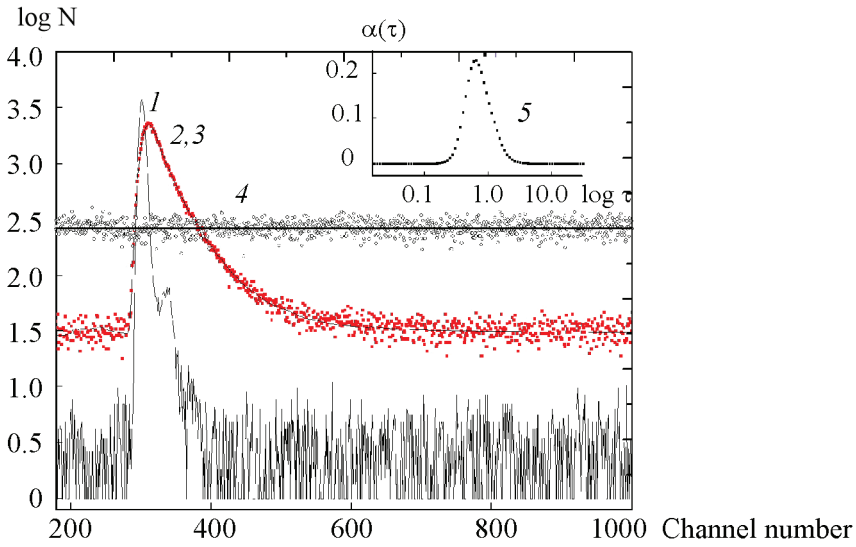

Fig. 1. Measurements and analysis of fluorescence decay kinetics of an aqueous solution of Th-C23 in the presence of AF (0.05 mg/mL) (λ_{fl} = 600 nm): time profile of exciting pulse (λ_{ex} = 467 nm), time per channel 0.036 ns (1); fluorescence decay curves (points, experimental; solid line, approximation of decay function by continuous distribution α(τ) given in the inset by curve 5) (2 and 3); distribution of relative differences corresponding to distribution α(τ) (4).

the results of such modeling. Representation of function α(τ) as a unimodal distribution with a maximum $\tau_0 \sim 1$ ns was observed to be adequate and was confirmed by the random nature of the distribution of relative differences $R(t)$.

Each distribution mode α(τ) was previously shown to correspond to a certain way of incorporating dye molecules into AF [11, 18]. It could be hypothesized in our instance that a single observed distribution mode α(τ) corresponded to a single way of incorporating Th-C23 dye into the AF structure, for which the molecules had a certain orientation relative to the fibril grooves. The degree of fluorescence polarization was measured to check this hypothesis and refine the geometry of the AF–dye complex.

Degree of fluorescence polarization of Th-C23. The degree of fluorescence polarization of ThT and other benzothiazole dyes was reported not to be an informative parameter because it was practically independent of the viscosity and rigidity of the fluorophore microenvironment [23, 24]. This occurred because the rotational relaxation time of a molecule, as a rule, is much longer than the torsional relaxation of its fragments relative to each other that leads to nonradiative deactivation, i.e., the molecules cannot substantially change their orientation during the time they exist in the excited state [23]. This results in the degree of fluorescence polarization of most MRs, including ThT and its derivatives, having the limiting high value in solvents of high and low viscosity and upon incorporation into biopolymer structures [23–26]. Figure 2 shows measured degrees of fluorescence polarization of the complex Th-C23 (5 μM) + AF (0.05 mg/mL) + ThT (6 μM), confirming that the degree of polarization of the complexed dye in solution was high within the whole fluorescence spectrum.

The fluorescence spectrum of ThT incorporated into AF and the absorption spectrum of Th-C23 overlapped significantly (Fig. 1, dashed line). Therefore, these dyes were a convenient donor–acceptor pair for studying energy transfer during their binding to AF. Both dyes were effectively incorporated into AF to form a complex with intense fluorescence. The absorption and fluorescence spectra of aqueous solutions of Th-C23 were studied after adding various concentrations of ThT to determine the possibility of forming a complex between free dye molecules and the effectiveness of energy transfer between them. A short-wavelength band with a maximum at 415 nm that corresponded completely to the absorption of an aqueous solution of free ThT appeared in the absorption spectrum (Fig. 3) upon increasing the ThT concentration, i.e., the absorption spectrum was a superposition of the individual dye spectra. The fluorescence quantum yield of Th-C23 was extremely low (~0.001), as before [15]. Addition of ThT did not cause a noticeable change in the fluorescence intensity of the Th-C23 solution at λ_{ex} = 420 nm (near the absorption maximum of ThT) and λ = 550 nm (the absorption band of Th-C23). Both dyes at the studied concentrations (1–10 μM) did not form a fluorescing complex in aqueous solution so energy transfer between the molecules did not occur.

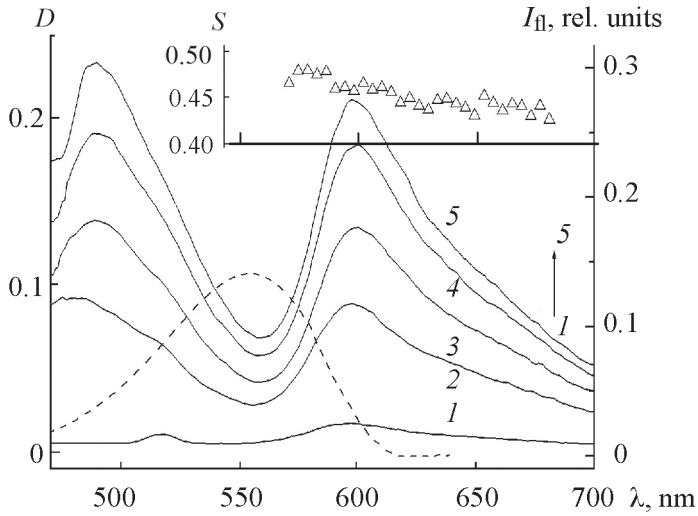

Fig. 2. Fluorescence spectra of an aqueous solution of the complex Th-C23 (5 μM) + AF (0.05 mg/mL) + ThT {[ThT] = 0 (1), 1 (2), 2 (3), 4 (4), and 6 μM (5)}; in the inset: points, dependence of degree of polarization *S* of fluorescence on wavelength of complex in the presence of ThT (6 μM), λ_{ex} = 440 nm; dashed line, absorption spectrum of aqueous solution of Th-C23 (4 μM) in the presence of AF (0.05 mg/mL) after subtracting Rayleigh scattering of the solution.

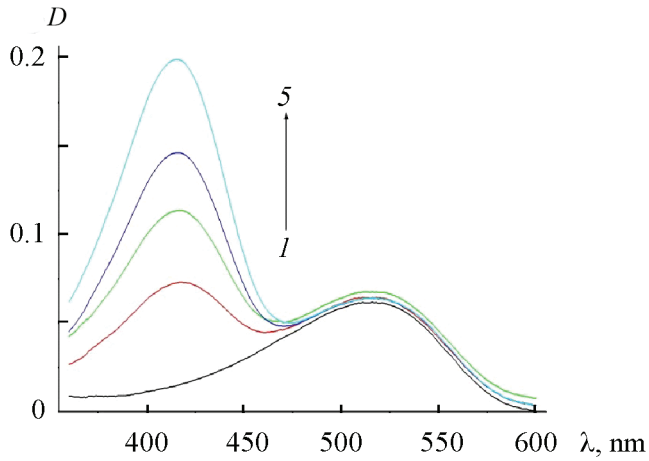

Fig. 3. Absorption spectra of an aqueous solution of Th-C23 (5 μM) with added ThT: 0 (1), 1 (2), 2 (3), 4 (4), and 6 μM (5).

Let us examine the measured fluorescence spectra of the complex (Th-C23–ThT) in the presence of AF in solution at λ_{ex} = 440 nm, corresponding to the ThT absorption spectrum maximum. The absorption of Th-C23 dye bound to AF was insignificant at this wavelength (Fig. 2). The fluorescence intensity at λ = 600 nm, corresponding to the emission maximum of the complex (Th-C23–AF), was low without ThT (Fig. 2). Addition to the solution of ThT (1.0 μM) caused the emission band of this dye (480 nm) to appear and the emission intensity of Th-C23 (600 nm) to increase five-fold. An increase in the ThT concentration led to a further increase of Th-C23 fluorescence. The fluorescence spectrum characteristically did not shift. Because the fluorescence spectrum of ThT incorporated into AF overlapped the absorption spectrum of the complex Th-C23–AF, the reason for the emission intensity increase was considered inductive-resonant transfer of excitation energy from ThT, the donor, to Th-C23, the acceptor. The fact that the fluorescence quantum yield of these dyes increased

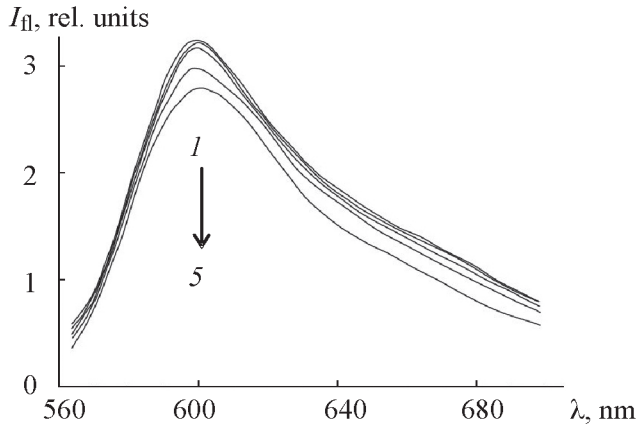

Fig. 4. Fluorescence spectrum of the complex Th-C23 (5 μM) + AF (0.05 mg/mL) + ThT {[ThT] = 0 (1), 1 (2), 2 (3), 4 (4), and 6 μM (5)}, λ_{ex} = 550 nm.

significantly upon their incorporation into AF promoted effective energy transfer. Energy transfer led to a decrease in the average donor fluorescence lifetime, which was confirmed experimentally, i.e., the average ThT fluorescence lifetime decreased from 1.28 to 0.87 ns.

A change in the ThT concentration led only to a characteristic insignificant decrease in the fluorescence intensity for λ_{ex} = 550 nm, which corresponded to the absorption maximum of the Th-C23–AF complex (Fig. 4). In our opinion, this was a consequence of some competition of the dye molecules for the incorporation site in the AF structure.

As a rule, acceptor fluorescence during energy transfer in solution is strongly depolarized [27]. However, the situation was different in our instance. As noted, the degree of fluorescence polarization of Th-C23 in the complex was high for λ_{ex} = 440 nm within the whole fluorescence spectrum, from 0.47 at the short-wavelength edge to 0.42 at the long-wavelength edge (Fig. 2). Because the main fluorescence intensity of Th-C23 at ThT concentration 5.0 μM and λ_{ex} = 440 nm was due to energy transfer, it should be recognized that this process in our instance did not lead to fluorescence depolarization. This was possible only if two conditions were fulfilled: 1) the donor and acceptor molecules were situated under rigid conditions; 2) the donor and acceptor transition moments were either parallel or antiparallel.

The inductive-resonant rate constants for transfer of electronic excitation energy could be determined from the relationship:

$$k = 1/\tau_D (R/R_0)^6 ,$$

where τ_D is the donor fluorescence decay lifetime in the absence of acceptor; R, the distance from donor to acceptor; R_0, the Forster transfer radius at which the transfer rate constant is equal to the radiative rate constant. The Forster radius expressed in Ångstroms was determined from the equation

$$R_0 = 8.8 \times 10^{-25}\, \kappa^2 q_D n^{-4} J .$$

Here, κ^2 is a factor considering the mutual orientation of the donor and acceptor molecules; q_D, the donor quantum yield in the absence of acceptor; n, the medium refractive index; J, the overlap integral considering overlap of the donor fluorescence spectrum and the acceptor absorption spectrum of energy:

$$J = \int_0^\infty F_D(\lambda)\varepsilon_A(\lambda)\lambda^4 d\lambda ,$$

where $F_D(\lambda)$ is the donor fluorescence spectrum normalized to unity; $\varepsilon_A(\lambda)$, the acceptor extinction coefficient corresponding to wavelength λ.

Various methods have been used to show that ThT molecules become planar upon incorporation into AF and are located along fibril grooves [28–30]. The fluorescence decay kinetics of ThT, which had a characteristic bimodal distribution,

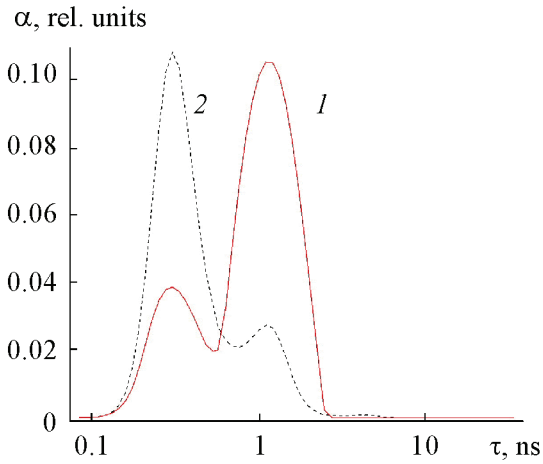

Fig. 5. Distribution α(τ) obtained by analyzing fluorescence decay curves of solutions of ThT (5.0 μM) + AF (0.05 mg/mL) (1) and ThT (5.0 μM) + AF (0.05 mg/mL) + Th-C23 (5.0 μM) (2); λ_{ex} = 407 nm, λ_{fl} = 490 nm.

were analyzed and refined using the Krebs model [28]. According to our results, most ThT molecules were incorporated into fibril grooves along the long axis. ThT molecules incorporated in this manner had very limited free internal rotation and a characteristically higher quantum yield and longer fluorescence lifetime. This was confirmed by measuring the degree of fluorescence polarization of ThT in stretched PVA films and AF [28]. The other probe molecules were incorporated into AF perpendicular to their long axis. In this instance, fragments of the probe molecules had free torsional motion, which led to a significant decrease in the quantum yield and fluorescence decay lifetime [18].

Orientational factor κ^2 significantly affected the energy-transfer efficiency and could vary from 0 to 4 depending on the mutual orientation of the donor and acceptor. Because the acceptor had a high degree of fluorescence polarization that was close to the limit, it was assumed in our instance that κ^2 = 4 (parallel orientation of donor and acceptor) or 1 (antiparallel orientation). Considering this, R_0 values of 54 and 68 Å were calculated. The calculations considered that ThT had two modes of incorporation into AF, for which the fluorescence quantum yields were 0.83 and 0.30 [31]. However, only molecules of the first mode, which were positioned along the grooves, were considered because dye molecules were oriented perpendicular to the grooves for the second mode. As shown previously, Th-C23 had only one mode of incorporation. The dye fluorescence quantum yield was 0.15. Also, two orientations of the donor and acceptor were examined, i.e., parallel and antiparallel (two possible values of R_0). The Forster radius of dipole–dipole energy transfer for the (ThT + AF) + Th-C23 system could vary in the range 54–68 Å. The given values were averages and could be refined using the measured donor fluorescence decay kinetics in the presence or absence of the acceptor.

The ThT fluorescence decay kinetics also varied because of energy transfer. Figure 5 shows distributions α(τ) obtained from an analysis of emission decay curves using the MEM. The decay mode without the acceptor in the solution had a characteristically longer lifetime and higher amplitude. The relative amplitude of the long-lived mode decreased in the presence of the acceptor (Th-C23), while that of the short-lived mode increased. This indicated that energy transfer was more characteristic of fluorophores with a long lifetime. Energy transfer was efficient because the donor and acceptor dipole moments were parallel to each other.

Conclusions. The fluorescence decay kinetics of styryl derivative Th-C23 intercalated in AF were non-exponential and could be represented as a unimodal distribution of fluorophores among decay lifetimes α(τ). This was indicative of one mode of incorporation of Th-C23 into AF.

The new ThT derivative Th-C23 was effectively incorporated into the AF structure, had a long-wavelength position of the absorption spectrum, and together with ThT formed a convenient donor–acceptor pair where ThT acted as the donor; Th-C23, as the acceptor of electronic excitation energy. The degree of acceptor fluorescence polarization was high and close to limiting despite the energy transfer. This led to the conclusion that the donor and acceptor molecules had a parallel or antiparallel mutual orientation. Based on inductive-resonant Forster energy-transfer theory, the critical transfer radius was determined and could vary from 54 to 68 Å depending on the mutual orientation and donor and acceptor quantum yield.

The research confirmed the previous hypothesis that ThT styryl derivatives were incorporated into AF grooves mainly along their long axis and opened possibilities for using inductive-resonant energy transfer to study the fibril structure and formation mechanism.

Acknowledgment. The work was financially supported by the Ministry of Education of the Republic of Belarus, GPNI [State Program for Scientific Research] "Photonics and electronics for innovation," Task 1.5.

REFERENCES

1. M. A. Haidekker, T. P. Brady, D. Lichlyter, and E. A. Theodorakis, *Bioorg. Chem.*, **33**, No. 6, 415–425 (2005); doi: 10.1016/j.bioorg.2005.07.005.
2. W. L. Goh, M. Y. Lee, Th. L. Joseph, S. T. Quah, Ch. J. Brown, Ch. Verma, S. Brenner, F. J. Ghadessy, and Y. N. Teo, *J. Am. Chem. Soc.*, **136**, No. 17, 6159–6162 (2014); doi: 10.1021/ja413031h.
3. V. I. Stsiapura, A. A. Maskevich, V. A. Kuzmitsky, V. N. Uversky, I. M. Kuznetsova, and K. K. Turoverov, *J. Phys. Chem. B*, **112**, No. 49, 15893–15902 (2008); doi: 10.1021/jp805822c.
4. N. Amdursky, R. Gepshtein Y. Erez, and D. Huppert, *J. Phys. Chem. A*, **115**, No. 12, 2540–2548 (2011); doi: 10.1021/jp1121195.
5. M. A. Haidekker, Th. P. Brady, D. Lichlyter, and E. A. Theodorakis, *J. Am. Chem. Soc.*, **128**, No. 2, 398–399 (2006); doi: 10.1021/ja056370a.
6. M. K. Kuimova, G. Yahioglu, J. A. Levitt, and K. Suhling, *J. Am. Chem. Soc.*, **130**, No. 21, 6672–6673 (2008); doi: 10.1021/ja800570d.
7. T. Ban, D. Hamada, K. Hasegawa, H. Naiki, and Y. Goto, *J. Biol. Chem.*, **278**, No. 19, 16462–16465 (2003); doi: 10.1074/jbc.C300049200.
8. S. A. Hudson, H. Ecroyd, T. W. Kee, and J. A. Carver, *FEBS J.*, **276**, No. 20, 5960–5972 (2009); doi: 10.1111/j.1742-4658.2009.07307.x.
9. H. Naiki, K. Higuchi, M. Hosokawa, and T. Takeda, *Anal. Biochem.*, **177**, No. 2, 244–249 (1989); doi: 10.1016/0003-2697(89)90046-8.
10. N. Yue, H. Fu, Y. Chen, X. Gao, J. Dai, and M. Cui, *Eur. J. Med. Chem.*, **243**, Article ID 114715 (2022); doi: 10.1016/j.ejmech.2022.114715.
11. G. Gorbenko, V. Trusova, E. Kirilova, G. Kirilov, I. Kalnina, A. Vasilev, S. Kaloyanova, and T. Deligeorgiev, *Chem. Phys. Lett.*, **495**, 4–6 (2010); doi: 10.1016/j.cplett.2010.07.005.
12. A. V. Lavysh, A. I. Sulatskaya, A. A. Lugovskii, E. S. Voropay, I. M. Kuznetsova, K. K. Turoverov, and A. A. Maskevich, *J. Appl. Spectrosc.*, **81**, No. 2, 205–213 (2014).
13. A. A. Maskevich, *Zh. Bel. Gos. Univ. Fiz.*, No. 2, 4–14 (2021).
14. A. A. Maskevich, *J. Appl. Spectrosc.*, **88**, 1125–1130 (2021).
15. E. I. Pligin, A. V. Lavysh, A. A. Lugovskii, E. S. Voropay, E. E. Kopishev, and A. A. Maskevich, *J. Appl. Spectrosc.*, **89**, No. 6, 205–213 (2022).
16. A. A. Maskevich, V. I. Stepuro, S. A. Kurguzenkov, and A. V. Lavysh, *Vesn. GrDzU imya Yanki Kupaly, Ser. 2, Mat. Fiz. Inf. Vylich. Tekh. Kirav.*, **159**, No. 3, 107–119 (2013).
17. V. I. Stepuro, *Vesn. GrDzU imya Yanki Kupaly, Ser. 2,* **5**, No. 1, 52–61 (2001).
18. A. A. Maskevich, V. I. Stsiapura, and P. T. Balinski, *J. Appl. Spectrosc.*, **77**, No. 2, 194–201 (2010).
19. A. K. Livesey and J.-C. Brochon, *Biophys. J.*, **52**, No. 5, 693–706 (1987); doi: 10.1016/S0006-3495(87)83264-2.
20. A. A. Maskevich, V. I. Stsiapura, V. A. Kuzmitsky, I. M. Kuznetsova, O. I. Povarova, V. N. Uversky, and K. K. Turoverov, *J. Proteome Res.*, **6**, No. 4, 1392–1401 (2007); doi: 10.1021/pr0605567.
21. P. K. Singh, M. Kumbhakar, H. Pal, and S. Nath, *J. Phys. Chem. B*, **114**, No. 17, 5920–5927 (2010); doi: 10.1021/jp100371s.
22. Y. Erez, Y.-H. Liu, N. Amdursky, and D. Huppert, *J. Phys. Chem. A*, **115**, No. 30, 8479–8487 (2011); doi: 10.1021/jp204520r.
23. I. M. Kuznetsova, A. I. Sulatskaya, A. A. Maskevich, V. N. Uversky, and K. K. Turoverov, *Anal. Chem.*, **88**, No. 1, 718–724 (2016); doi: 10.1021/acs.analchem.5b02747.
24. M. Groenning, *J. Chem. Biol.*, **3**, No. 49, 1–18 (2010); doi: 10.1007/s12154-009-0027-5.
25. A. A. Maskevich, *Vesn. GrDzU imya Yanki Kupaly, Ser. 2, Mat. Fiz. Inf. Vylich. Tekh. Kirav.*, **10**, No. 1, 83–92 (2021).

26. R. Sabate and S. Saupe, *Biochem. Biophys. Res. Commun.*, **360**, 135–138 (2007); doi: 10.1016/j.bbrc.2007.06.063.
27. L. V. Levshin and A. M. Saletskii, *Luminescence and Its Measurements: Molecular Luminescence* [in Russian], MGU, Moscow (1989), pp. 159–165.
28. M. R. H. Krebs, E. H. C. Bromley, and A. M. Donald, *J. Struct. Biol.*, **149**, No. 1, 30–37 (2005); doi: 10.1016/j.jsb.2004.08.002.
29. A. A. Maskevich, S. A. Kurhuzenkau, A. V. Lavysh, L. N. Kivach, and S. A. Maskevich, *J. Appl. Spectrosc.*, **82**, No. 4, 532–539 (2015).
30. Ch. Wu, Zh. Wang, H. Lei, Y. Duan, M. T. Bowers, and J.-E. Shea, *J. Mol. Biol.*, **384**, No. 3, 718–729 (2008); doi: 10.1016/j.jmb.2008.09.062.
31. A. I. Sulatskaya, A. A. Maskevich, I. M. Kuznetsova, V. N. Uversky, and K. K. Turoverov, *PLoS One*, **5**, No. 10, Article ID e15385 (2010); doi: 10.1371/journal.pone.0015385.